Post-natal development of the Reeler mouse cerebellum: An ultrastructural stud

UNIVERSITÀ DEGLI STUDI DI TORINO

Post-natal development of the Reeler mouse cerebellum:An ultrastructural study

Claudia Castagna[a,*], Patrizia Aimar[a], Silvia Alasia[a], Laura Lossi[b]

[a] University of Turin, Department of Veterinary Sciences, Italy
[b] INN Istituto Nazionale di Neuroscienze, Italy

∗ Corresponding author at: Via Leonardo da Vinci 44, I-10095 Grugliasco, TO, Italy.
Tel.: +39 0116709128.
E-mail address: claudia.castagna@unito.it (C. Castagna).

Summary Reelin, an extracellular protein promoting neuronal migration in brain areas with a laminar architecture, is missing in the Reeler mouse (reelin$^{-/-}$). Several studies indicate that the protein is also necessary for correct dendritic outgrowth and synapse formation in the adult forebrain.

By transmission electron microscopy, we characterize the development and synaptic organization of the cerebellar cortex in Reeler mice and wild type control littermates at birth, postnatal day (P) 5, 7, 10 and 15. Ultrastructural analysis shows deep alterations in cortical architecture and mispositioning of the Purkinje neurons (Pns), which remain deeply embedded in a central cellular mass within the white matter, with highly immature features. Quantitative examination shows that Reeler mice display: (i) a lower density of granule cells and a higher density of Pns, from P10; (ii) a lower density of synaptic contacts between Pn dendrites and parallel or climbing fibers, from P5; (iii) a lower density of synaptic contacts between basket cells and Pns, from P5; and (iv) a lower density of mossy fiber rosettes, from P10.

Our results demonstrate that Reelin profoundly affects the structure and synaptic connectivity of post- natal mouse cerebellum.

Keywords: Reeler Cerebellum Ultrastructure Mouse Synapse Purkinje neurons Development

1. Introduction

Several mouse mutations that affect the cerebellum have been thoroughly studied. In Reeler, the first described of these mutations (Falconer, 1951), the Purkinje neurons (Pns) fail to migrate properly and remain largely situated in ectopic clusters deep in the cerebellar anlage that ultimately grows into a hypoplastic cerebellum (Rice and Curran, 1999). Several decades after the first description of the Reeler phenotype, the mutated protein was discovered and named Reelin, according to the typical alterations in gait that characterized recessive homozygous mice (reelin$^{-/-}$) where the protein was totally defective (D'Arcangelo et al., 1995). It was subsequently demonstrated that Reelin is the first molecule of a complex intra- cellular cascade that regulates neuronal migration (reviewed in D'Arcangelo and Curran, 1998; Lambert de Rouvroit and Goffinet, 1998).

Anatomical anomalies in the Reeler mouse can be observed in a number of different areas of the central nervous system (reviewed in Katsuyama and Terashima, 2009). In the spinal cord,

nociceptive pathway neurons and preganglionic sympathetic and parasympathetic neurons are affected. In the brain, several areas and/or neuronal populations are hit by the mutation including the olfactory bulb, neocortex, hippocampus, a number of nuclei associated with the encephalic nerves, the pontine nuclei, inferior olivary nucleus, anterior colliculus, substantia nigra, and the cerebellum.

Gross anatomy and light microscopy studies have described the anomalies in reelin$^{-/-}$ mouse cerebellum in detail. Macroscopically, only very shallow notches, which are probably the remnants of a tentative foliation, are visible at its surface (Mikoshiba et al., 1980). The thickness of the molecular layer (ML) is irregular, and only 5% of Pns were observed between the molecular and granular layers, 10% were in the granular layer, and the rest were ectopically localized in a central cellular mass intermingled with the white matter (Mariani et al., 1977; Heckroth et al., 1989; Yuasa et al., 1993). Electrophysiologically, Pns in the piriform layer and those in the granular layer display an all-or-nothing response to stimulation, whereas those in the central cellular mass exhibit stim- ulus intensity-graded responses, indicating that the first receive a single climbing fiber (as in wild type), while the others receive a convergent input from several climbing fibers (Mariani et al., 1977). The abnormal physiological maturation of Pns has also been confirmed, albeit indirectly, in a reelin-related HT3A recep- tor knockout mouse (Oostland et al., 2013). The granular cells form a layer beneath the ML, but at a lower density than the normal counterpart, as a consequence of a reduced proliferation largely owing to cerebellar atrophy (D'Arcangelo and Curran, 1998). Finally, the Bergmann glia are ectopically localized, with fibers sometimes descending in a reversed direction (Terashima et al., 1985).

Despite these studies, limited information is available on the post-natal development of the reelin$^{-/-}$ cerebellum at the ultrastructural level compared to other CNS areas such as cerebral cortex and hippocampus (Borrell et al., 1999; Yabut et al., 2007; Niu et al., 2008; Hellwig et al., 2011; Ventruti et al., 2011).

2. **Materials and methods**

2.1. Animals

Studies were performed on 20 mice. Animals ranged in age from birth (P0) to postnatal day 15 (P15). All experiments were carried out according to Italian and EU regulations on animal welfare (DLS 116/92) and were authorized by the Italian Ministry of Health and the Bioethics Committee of the University of Turin. The number of animals used was kept to a minimum and all efforts were made to minimize their suffering. In addition, although not prescribed by national regulations, all animal procedures were carried out according to the guidelines and recommendations of the European Union (Directive 2010/63/UE). All animals were genotyped according to current protocols to ascertain their genetic background before being used in this study (D'Arcangelo et al., 1996).

2.2. Histology and ultrastructural analysis

Qualitative analysis was carried out on Reeler mice at P0, P5, P7, P10 and P15. For quantitative studies P0, P5, P10 and P15 Reeler and littermate wild-type (WT) mice were used (n = 4/each post- natal age). After the animals were euthanized intraperitoneally with sodium pentobarbital (30 mg/kg), they were perfused with 2% glutaraldehyde + 1% paraformaldehyde in Sörensen buffer 0.1 M pH 7.4. Two hundred μm thick parasagittal vibratome slices of the vermis were then cut and processed according to standard TEM procedures.

For quantitative analysis, a single ultrathin parasagittal section of the entire vermis was collected onto a 75 mesh grid to reduce the tissue areas covered by grid bars as much as possible. Due to the small cerebellar size, the area of the grid was sufficient to host the entire cerebellar section at all ages examined both in Reeler and WT mice. Objects (neuronal cell bodies or synapses) were counted at a magnification of 8700× over an area of 8008 μ^2 selected at the lower left corner of each mesh of the grid occupied by tissue. Two different ultrathin sections from the same animal, collected at a distance of at least 200 μm (to avoid recounting of the same Pns) along the transverse plane were subjected to analysis.

2.3. Statistics

Results obtained from each section pair from one respective mouse were subjected to statistical analysis using a Student's t- test. In all cases there were no statistically significant differences in measurements from sections belonging to the same animal, and thus their values were averaged and the mean used for statistical analysis. A paired Student's t-test was used to compare the averaged values obtained for each animal of the same group and between groups. Results were considered statistically significant with $p \leq 0.05$.

3. Results

The main alterations in the architecture of the Reeler cerebellum could also be appreciated in reconstructions of semi-thin sections from oriented plastic-embedded parasagittal sections prepared for subsequent ultrastructural examination (Fig. 1).

3.1. Ultrastructure of the postnatal Reeler cerebellum

3.1.1. Postnatal day 0

The surface of P0 Reeler cerebellum comprised several layers of densely packed granular cells forming an external granular layer (EGL) with features similar to those observed in WT mice (Figs. 1A and 2A). Mitotic granular cells were also evident, more frequently in close apposition to the pial surface (Fig. 2B). In general, the EGL abruptly disappeared at the level of the choroidal plexus (posterior) showing instead a normal extension in proximity of the posterior colliculus (anterior).

Deep to the EGL, a rudimentary ML was visible with scattered clusters of parallel fibers separated by wide electron-lucent spaces (Fig. 2A and C). Interspersed between the parallel fibers, migrating granule cells could easily be recognized (Fig. 2A). Rare profiles intermingled with the parallel fibers containing clusters of large vesicles, which are typical of growing dendrites. They only rarely received a primitive synaptic contact from a parallel fiber terminal (Fig. 2D). Among the parallel fibers, rare elongated profiles of small dendrites were also visible (Fig. 2E). The Reeler internal granular layer (IGL) consisted of loosely grouped cells of various size and ultrastructure, (Figs. 1A and 2F). The larger cells were immature Pns. Pns contained abundant cytoplasm with discrete cytoplasmic organelles and typical membrane specializations, commonly referred to as hypolemmal cisternae. The hypolemmal cisternae consisted of a mitochondrion in close apposition to a fused subsurface cistern running parallel to the cellular membrane, opposite to the light glial limiting membrane (Fig. 2H). The surface of the cell body was generally devoid of synaptic contacts, with the exception of sporadic small pre-synaptic profiles containing clear, small round vesicles and a hint of asymmetrical thickening (Fig. 2G and I). When observed at higher magnification, many of the large immature Pns showed the presence of numerous dendritic growth cones on their surface (Fig. 2J). The IGL also displayed wide intercellular spaces and a few unmyelinated fibers with an irregular outline, many of them containing clusters of very large vesicles (Fig. 2F and G).

3.1.2 Postnatal day 5

A low magnification view of the cerebellar cortex in WT (Fig. 3A) and Reeler (Figs. 1B and 3B) littermates displayed striking ultra- structural differences between the two phenotypes in the thickness of the EGL and positioning of the Pns.

At higher magnification, the parallel fibers were more compact than at P0 (Fig. 4A). They formed bundles separated by dendrites and glial sheets intermingled with small dendrites originating from the Pns. The membrane appositions of the axo-dendritic contacts between these two neuronal types displayed a 1:1 ratio typical of immature synapses, with a fairly short and straight apposition. Other more prominent dendrites displayed elongated profiles of small and medium size that were disorganized with respect to direction toward the pial surface. They were characterized by a clear section with some filaments and vesicles, and sporadic mitochondria (Fig. 4B). Axonal contacts with these dendrites were also visible, corresponding to the first immature climbing fiber synapses (Fig. 4B). Comparison with controls demonstrated that dendritic arborization originating from the Pns was more developed and better patterned in the ML of WT mice.

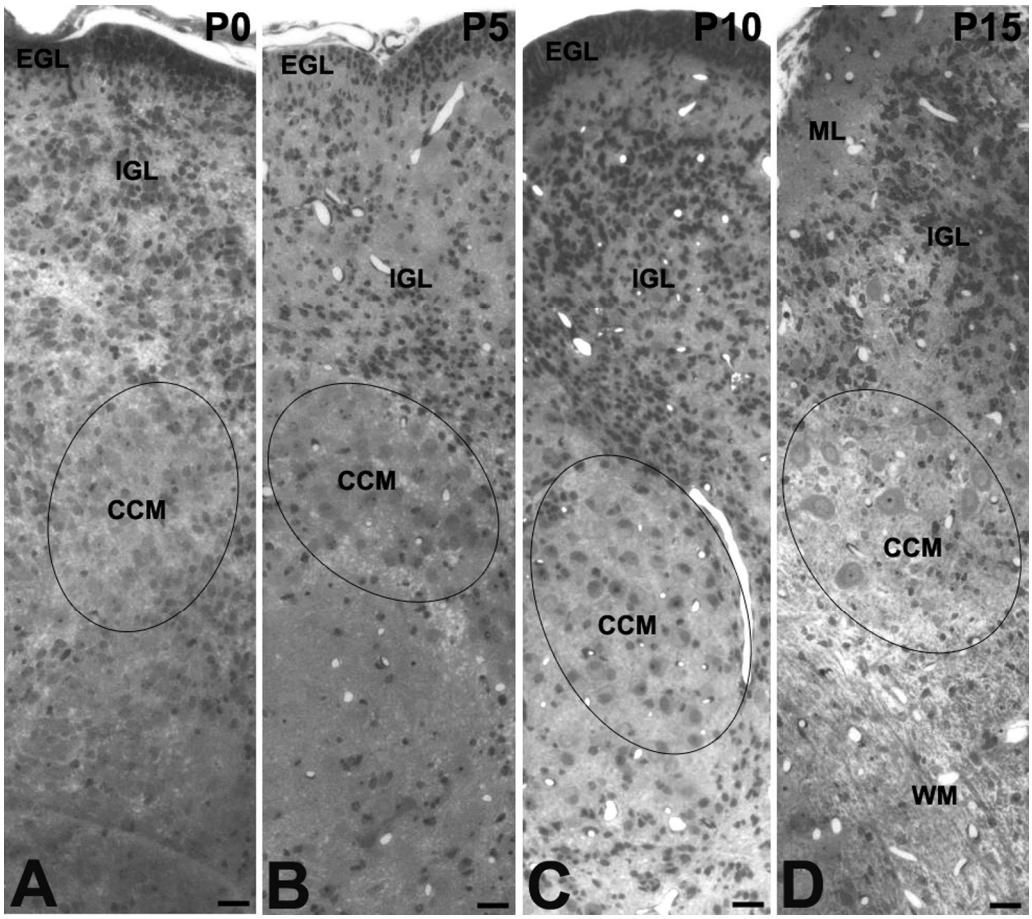

Fig. 1. Architecture of the Reeler cerebellum in toluidine blue stained semi-thin parasagittal sections cut through the vermis. With age, note the progressive disappearance of the EGL, the relative constancy in thickness and hypocellularity of the IGL, and the enlargement in size of the central cellular mass made by Purkinje neurons. Abbreviations: CCM, central cellular mass; EGL, external granular layer; IGL, internal granular layer; ML, molecular layer; P, postnatal day; WM, white matter. Bars = 125 μm.

The IGL (Figs. 1B, 3B, and 4C–G) contained neurons and glial cells, surrounded by a neuropil characterized by numerous fibers, some of which were beginning to develop a myelin sheath. Pns were clearly distinguishable by their larger size and ultrastructural features (Fig. 4C). However, only very few elements had a clear polarization such as the one shown in Fig. 4C. It is worth noting that in Reeler not only the polarization of the Pns was by far less evident than in controls, but that even when such a polarization was attained, an aberrant orientation of the cellular axis was common. Only rare Pns were normally positioned at the border between the ML and the IGL.

The axo-somatic contacts made by basket cells to the Pns were characterized by roundish and irregular clear vesicles of differing sizes (Fig. 4E). The synaptic apposition was discontinuous and symmetrical, faintly marked and without vesicles adhering to the presynaptic membrane. The more frequently observed axo-somatic contacts formed by climbing fibers were characterized by clusters of vesicles adhering to the presynaptic membrane. They contained numerous small clear round vesicles and a few medium-sized vesicles, and displayed a limited asymmetric synaptic

thickening (Fig. 4F).

The remaining IGL cells were of small to medium size, the smallest being post-migratory granule cells (Figs. 1B and 3B). The neuropil contained the first mossy fiber rosettes (Fig. 4G).

3.1.3. Postnatal day 7

The surface of the P7 Reeler cerebellum was smooth or only slightly indented, differing from controls where foliation was clearly appreciable. The EGL was still well recognizable (Fig. 5A). Differing from WT mice, the laminae of radial glia were discontinuous (Fig. 5B). Nonetheless, migrating granule cells were also present in the areas devoid of radial glia and did not present obvious ultrastructural differences from the same cells located in the areas where the radial glia developed normally.

The ML (Fig. 5A and D) and IGL (Fig. 5E and F) were characterized by a notable degree of immaturity and a much lower number of cells compared to WT littermates. Immaturity of the Reeler ML mainly affected the parallel fibers and their synapses with Pn dendrites (Fig. 5C). The size of the presynaptic element in these contacts was always larger than the postsynaptic counterpart, and the parallel fiber had a tendency to surround the postsynaptic dendrite, so that a synaptic concavity faced the presynaptic element (Fig. 5C). Occasional synaptic contacts attributable to climbing fibers could also be seen. Rare basket cells populated the innermost part of ML. They were of medium-size, with a clear nucleus filled with a finely granular material, and up to two nucleoli. Their cytoplasm was fairly well developed and elongated with the long axis directed parallel or almost parallel to the pial surface (Fig. 5A). Other rare cells in the same location had a polygonal boundary and scant cytoplasm (Fig. 5A), and were identified as primitive stellate neurons.

In the IGL, post-migratory granule cells were easily recognized. Other cells (Fig. 5E) were also easy to identify as they possessed the ultrastructural features already described for Pns at P5. The Golgi cells (Fig. 5F) could, at times, be recognized as rare elements deeply embedded in the central cellular mass. Still, additional cells displayed features of immaturity. A striking feature of the Reeler IGL/cellular mass was the presence of numerous mitoses (Fig. 5F). The rosettes made by the mossy fibers were well visible, albeit still primitive.

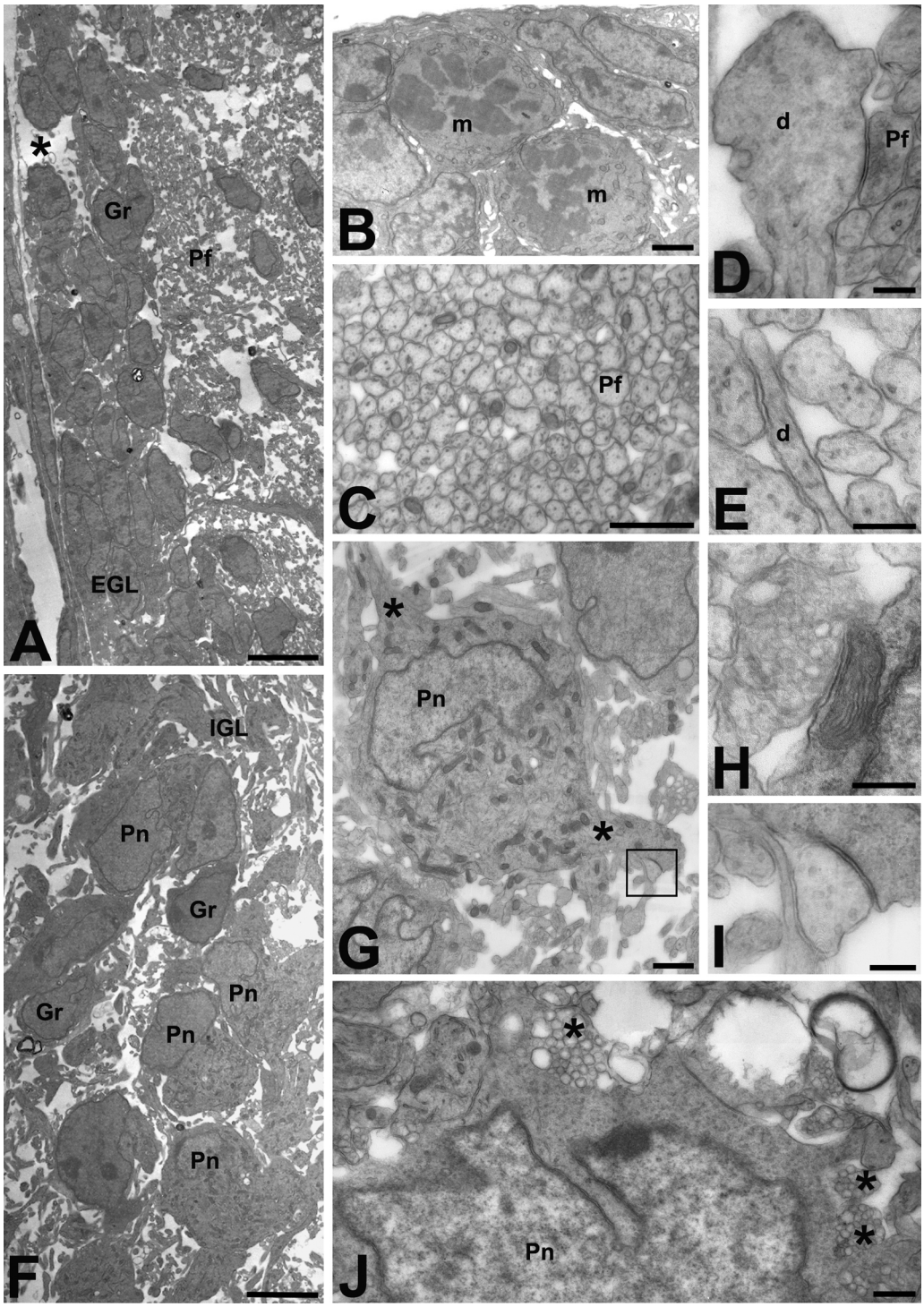

Fig. 2. Ultrastructure of the Reeler cerebellum at P0. (A) At the pial surface (left side of figure), granule cells (**Gr**) are organized into a rather compact external granular layer (**EGL**) that is, at times, interrupted by wide intercellular spaces, one of which is indicated by the asterisk. Below the EGL, a rudiment of the forming molecular layer is apparent with bundles of parallel fibers (**Pf**). Bar = 5 μm. (B) Mitotic granule cells (**m**) in the EGL. Bar = 2 μm. (C) A compact bundle of transversely cut parallel fibers with features similar to those observed in wild-type mice. Bar = 1 μm. (D) Immature synaptic contact between a parallel fiber terminal (**Pf**) and a growing dendritic tip (**d**) of a Purkinje neuron (**Pn**). The synaptic specialization displays a moderate degree of electron density. Bar = 250 nm. (E) Long and thin dendrite (**d**) surrounded by several parallel fibers in the molecular layer. Bar = 250 nm. (F) Area of

transition between the internal granular layer (**IGL**) and the deeper cerebellum (the pial surface is on the left side of the picture). Note the presence of several Pns intermingled with a few post-migratory granule cells (**Gr**) and wide intercellular spaces. Bar = 5 μm. (G) Cytological features of an immature Purkinje neuron: the cell organelles are dispersed throughout the cytoplasm without obvious polarization. Two main processes (asterisks) stem from the cell body. The area indicated by the rectangle is shown at higher magnification in (I). Bar = 1 μm. (H) Hypolemmal cistern – a typical membrane specialization – at the cell membrane of a Purkinje neuron. Bar = 250 nm. (I) Synapse received at the emergence of one of the two main processes of the Purkinje neuron in (G). Bar = 250 nm. (J) Dendritic growth cones (asterisks) at the surface of a Purkinje neuron (**Pn**) are characterized by an accumulation of large clear vesicles and vacuoles. Bar = 500 nm. Abbreviations: d, dendrite; EGL, external granular layer; Gr, granule cell; IGL, internal granular layer; m, mitosis; P, postnatal day; Pf, parallel fiber(s); Pn, Purkinje neuron.

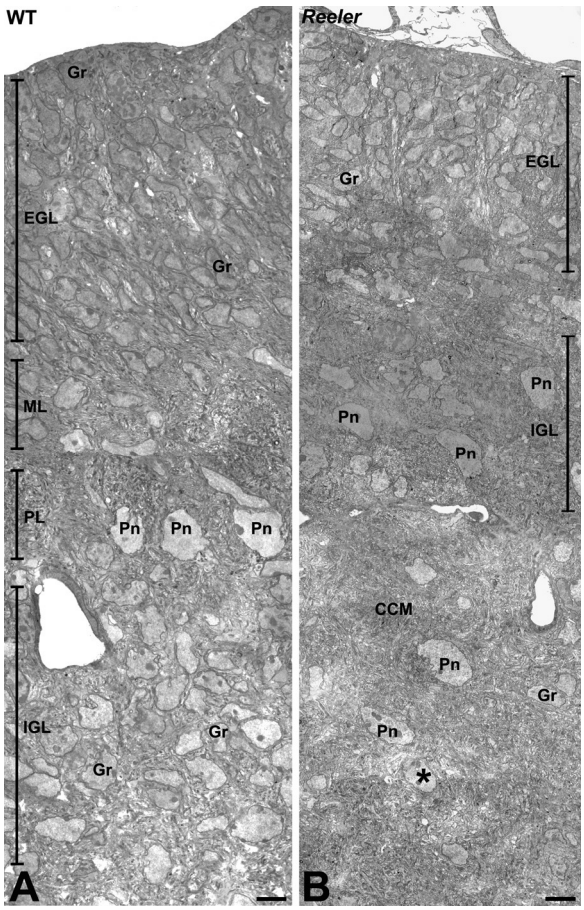

Fig. 3. Ultrastructure of the P5 cerebellum in wild-type (WT, A) and Reeler (B) mice. Low magnification micrographs of parasagittal sections of the vermis in normal and mutant mice show obvious differences in the architecture and ultrastructure of the developing cerebellar cortex. The superficial external granular layer (**EGL**) is far more developed and thicker in WT mice, and consists in a dozen or more layers of granule cells (**Gr**). The thickness of the EGL of the Reeler mouse is reduced to about one half, and the mutant cerebellar cortex is poorly differentiated and lacks the primordial molecular layer (**ML**) that is instead already visible in control mice. In the latter, the Purkinje neurons (**Pn**) start being organized in a monolayer at the border between the ML and the internal granular layer (**IGL**), forming a primordial piriform layer (**PL**) while, in Reeler, they are interspersed with numerous other cells of similar sizes and appearance. Some of these cells can be identified as granule cells (**Gr**), but many still display a high degree of immaturity and are thus difficult to identify with certainty on the basis of their ultrastructural features. A well-defined IGL is present in WT mice, consisting of more loosely packed granule cells (**Gr**) interspersed with some intermediate sized neurons and separated by clear intercellular spaces, whereas the corresponding area of the Reeler is

occupied by a central cellular mass (**CCM**) and appears hypocellular with only a few Purkinje neurons. In (B) the asterisks indicate a probable deep nucleus neuron. Abbreviations: CCM, central cellular mass; EGL, external granular layer; Gr, granule cell; IGL, internal granular layer; ML, molecular layer; P, postnatal day; PL, piriform layer; Pn, Purkinje neuron. Bars = 5 μm.

3.1.4. Postnatal day 10

The surface of the Reeler cerebellum was only slightly indented, different from controls in which the foliation was complete. The EGL was present, but much reduced in thickness (Fig. 1C). Synapses made by the parallel fibers in Reeler displayed a marked under- development of the glial lamina (Fig. 6B). The Pn dendrites were slightly more differentiated than at P7 with some branches that occasionally had spines. On their surface, the axo-dendritic contacts of the climbing and the parallel fibers were well visible (Fig. 6B and C).

The ultrastructural phenotype of a WT (Fig. 6D) and a Reeler (Fig. 6E) Pn is shown for comparison: it is immediately apparent that while the former displayed a typical polarized appearance of the cytoplasm with an overall piriform contour, the other was unpolarized and with a less pronounced oval shape. In Reeler, the Pns very rarely displayed processes and small spines (Fig. 6F). The soma of the Pns displayed a series of contacts from basket cells (Fig. 6G) or climbing fibers (Fig. 6H). The profound degree of ectopia of the Pns was aggravated at P10. In the central cellular mass, post- migratory granule cells (Fig. 6E) and, more rarely, a very few Golgi neurons were easily observed. Intermingled between them, the neuropil contained many glomeruli (Fig. 6I).

3.1.5. Postnatal day 15

The EGL was further reduced in thickness (Fig. 1D). The parallel fibers were now tightly packed and grouped in more or less regular bundles irregularly separated by Pn dendrites of differing size and orientation (Fig. 7C and D). Small Pn dendrites displayed highly asymmetric synaptic contacts with the parallel fibers (Fig. 7A). Occasionally, certain profiles had the typical mature arrangement of this type of contact, i.e. the two synaptic partners were concentrically arranged with an outside parallel fiber varicosity surrounding the inner dendritic spine (Fig. 7B). However, the surface of medium- size Pn dendrites remained rather smooth (Fig. 7C). The synaptic contacts made by terminals of the climbing fibers onto the dendritic shafts were clearly recognized (Fig. 7C). Basket and stellate cells were clearly recognizable (Fig. 7D), and a few migrating granule cells occupied the deeper part of the ML (Fig. 1D).

The ultrastructure of the IGL/central cellular mass (Figs. 1D and 7) was, for the most, similar to that described at P10.

3.2. Quantitative studies

Quantitative analysis was carried out in P0, P5, P10 and P15 mice (Fig. 8).

The density of the cerebellar granule cells (Fig. 8A) was calculated independently of their position in the EGL or the IGL. Starting from P10, WT mice displayed a significantly higher number of granule cells/area reaching values of about one-and-one-half times those seen in Reeler. In the P0–P5 interval, densities of the granule cells were not statistically different between the two genotypes. The density of Pns (Fig. 8B) was also calculated independently of their position in the different layers of the cerebellar cortex or the central cellular mass. It was noticeable that, whereas in the P0–P5 interval there was no statistically significant difference between WT and Reeler littermates, in the P10–P15 interval mutant mice displayed a significantly higher density of Pns compared to con- trols (about two-fold). Also, it was of interest that the reduction in density of the Pns in Reeler mice was statistically significant only when comparing P0 and P15 animals.

Contacts made by the parallel fibers onto Pn dendrites (Fig. 8C) and spines (Fig. 8D) were significantly lower density in Reeler, with the exception of those made on plain dendritic shafts at P5 (Fig. 8C). Notably, in the P5–P10 interval the density of the latter type of contacts significantly increased in both control and mutant mice. However, after substantial stability from P5 to P10, they continued to increase in WT mice only. Also in the case of Pn dendritic spines, WT mice displayed a significantly higher density of synapses than their mutant counterparts (Fig. 8D).

The density of synapses made by climbing fibers onto Pn dendrites (Fig. 8E) and somata (Fig. 8F) reached higher figures in WT mice than in Reeler from P5 onwards. The temporal trend followed a biphasic curve with a first increase in the P0–P5 interval, followed by substantial stability up to P10, and a second rise between P5 and P15 ($p < 0.05$; Fig. 8E). The trend in synaptic densities of the axo-somatic contacts (Fig. 8F) was more variable, with statistical significance between the two genetic backgrounds at P0 and P10 in favor of the controls, and a clear numerical reduction from P5 to P15 that was paralleled, in Reeler, only between P5 and P10.

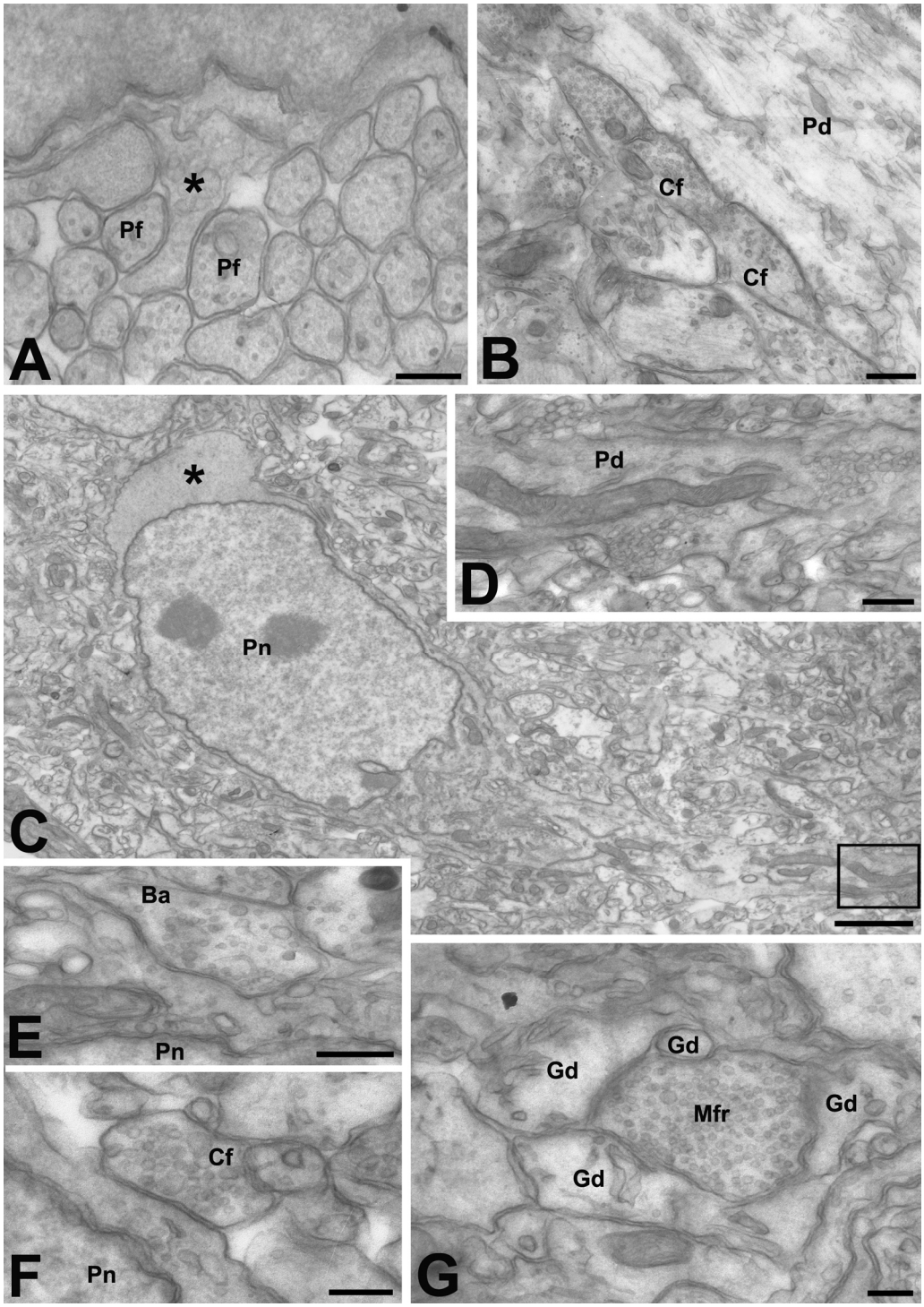

Fig. 4. Ultrastructure of the Reeler cerebellum at P5. (A) Bundle of parallel fibers two of which (**Pf**) are in contact with a spine on a cell body (asterisk). The spine has a smooth surface and is not yet surrounded by the parallel fiber terminals. Bar = 250 nm. (B) Climbing fiber-Purkinje neuron synapse. A relatively large Purkinje neuron dendrite (**Pd**) is contacted by the terminals of a climbing fiber (**Cf**). Bar = 500 nm. (C) Rare example of a well differentiated Purkinje neuron (**Pn**) in Reeler cerebellar cortex. The cell shows an evident polarization with an area of cytoplasm that is completely devoid of organelles (asterisk) and which will eventually give rise to the axon hillock, and, at the opposite pole, the emerging main dendritic trunk. The area in the rectangle is shown at higher magnification in (D).

It is noteworthy that, despite proper cytological maturation, this neuron is not properly aligned with respect to cortical lamination since the main dendrite is parallel rather than perpendicular to the pial surface of cerebellum. Bar = 2 μm. (D) The initial track of the main dendrite (**Pd**) of the Purkinje neuron shown in (C) is characterized by the presence of very long mitochondria and numerous vesicles. Bar = 500 nm.

(E) Axo-somatic synapse made by a basket cell (**Ba**) onto a Purkinje neuron (**Pn**). This type of synapse is characterized by clear, roundish and irregular vesicles of different sizes and a discontinuous symmetrical synaptic thickening. Bar = 500 nm. (F) Axo-somatic synapse made by a climbing fiber (**Cf**) onto a Purkinje neuron (**Pn**). This type of synapse is characterized by clear round clustered vesicles of different sizes and an asymmetrical synaptic thickening. Bar = 250 nm. (G) A rudimental glomerulus is formed by a central rosette (**Mfr**) – the projection of a mossy fiber – surrounded by several granule cell dendrites (**Gd**). The profile of the rosette is smoother than in wild-type mice. Bar = 250 nm. Abbreviations: Ba, basket cell; Cf, climbing fiber; Gd, granule cell dendrite (claw); Mfr, mossy fiber rosette; P, postnatal day; Pf, parallel fiber(s); Pd, Purkinje neuron dendrite; Pn, Purkinje neuron.

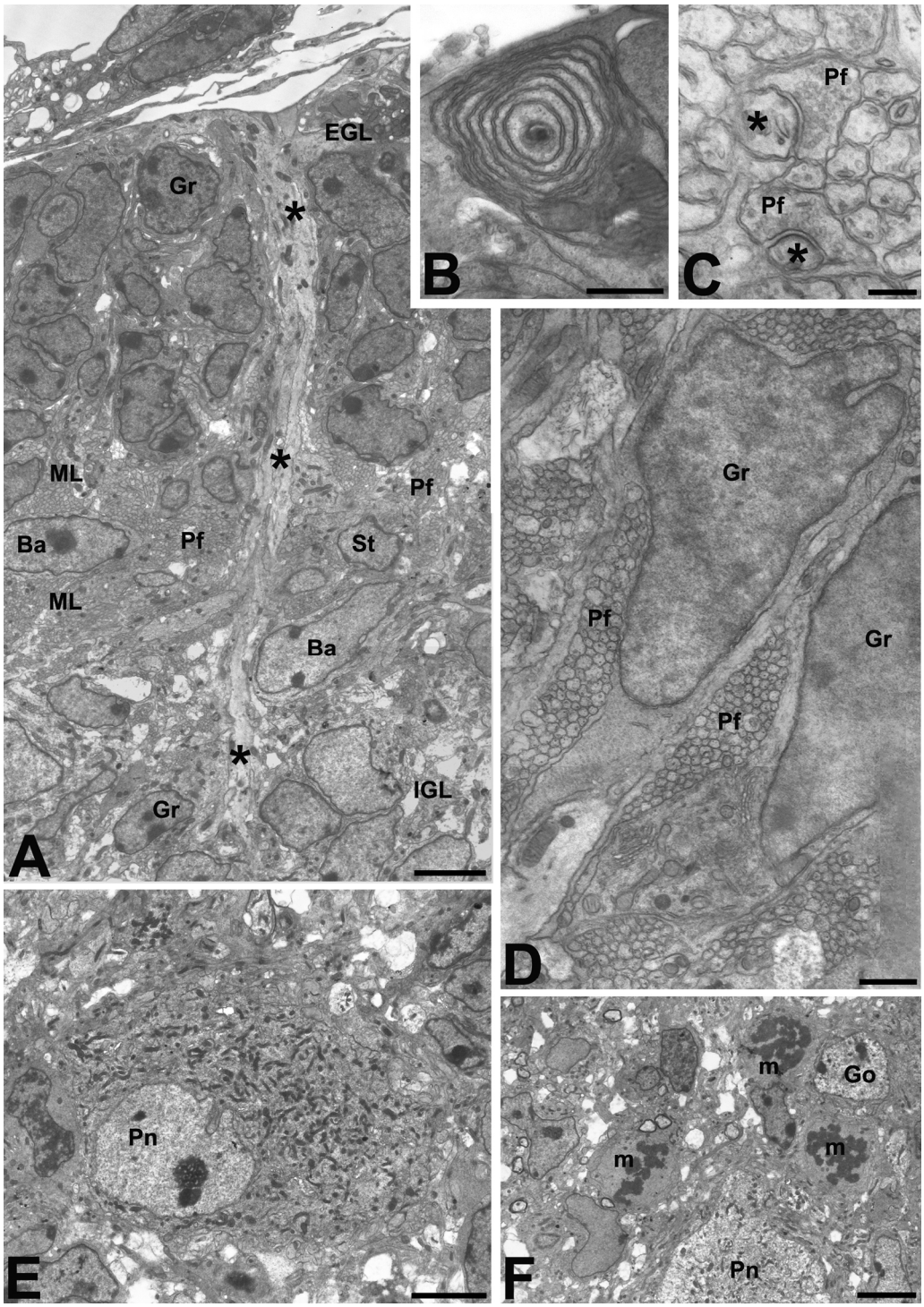

Fig. 5. Ultrastructure of the Reeler cerebellum at P7. (A) Low magnification view of the superficial cerebellum encompassing the external granular layer (**EGL**), molecular layer (**ML**) and the transition to the internal granular layer (**IGL**). Granule cells (**Gr**) in the EGL are organized in three clusters, two of which are separated by a radial glia lamina (asterisks). The ML contains bundles of parallel fibers (**Pf**) and a few cells. Two basket cells (**Ba**) and one primitive stellate neuron (**St**) can be identified on the basis of their size and cytological features. Bar = 5 μm. (B) Subpial pedicle of radial glia displaying a well differentiated ultrastructure. Bar = 250 nm. (C) Two synapses between Purkinje cell dendrites (asterisks) and parallel fibers (**Pf**) show a higher degree of maturity and the Pf begin to surround the postsynaptic dendrites. Bar = 500 nm.

(D) ML with two migrating granule cells (**Gr**) intermingled between bundles of parallel fibers (**Pf**). Bar = 1 μm. (E) Immature Purkinje neuron in the area occupied by the central cellular mass. Bar = 5 μm. (F) Superficial part of the IGL displaying three mitoses (m), one Golgi cell (**Go**) and a Purkinje neuron (**Pn**). Bar = 5 μm. Abbreviations: Ba, basket cell; EGL, external granular layer; Go, Golgi neuron; Gr, granule cell; IGL, internal granular layer; m, mitosis; ML, molecular layer; P, postnatal day; Pd, Purkinje neuron dendrite; Pf, parallel fiber(s); Pn, Purkinje neuron; St, stellate neuron. The density of the synapses between the mossy fiber rosettes and the granule cell claws (Fig. 8G) was not statistically dif- ferent at P5, but became significant at more advanced stages (P10, $p < 0.01$; P15, $p < 0.05$). It is worth observing that under both genotypic conditions, there was a significant increase in synaptic densities at glomeruli between P10 and P15 (controls $p < 0.05$; Reeler $p < 0.01$). Finally, the number of axo-somatic synapses made by the basket cells onto the Pn somata per unit area (Fig. 8H) was, again, significantly reduced in Reeler.

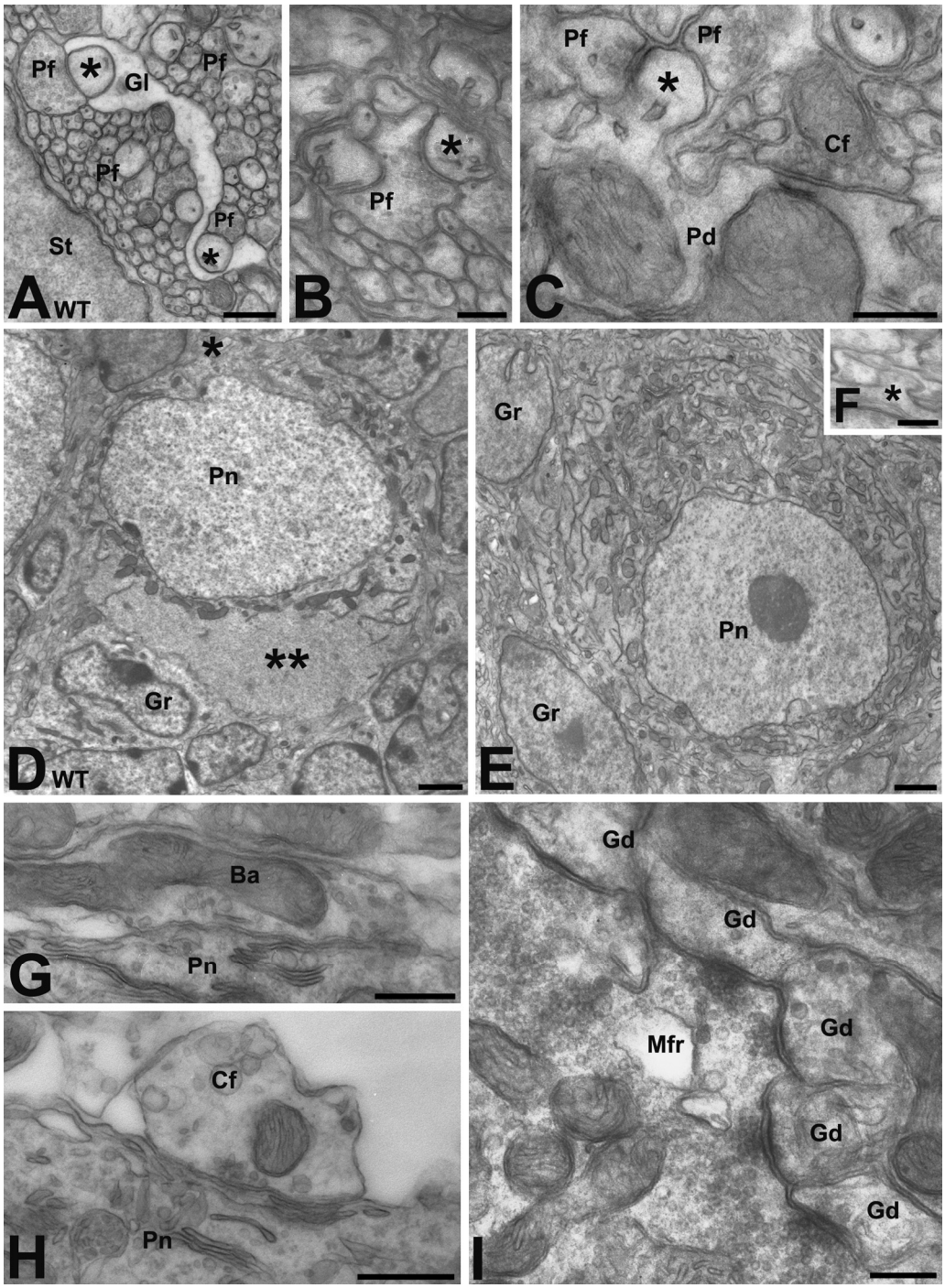

Fig. 6. Ultrastructure of the Reeler cerebellum at P10. (A and B) Comparison of the aspect of a axo-dendritic synapse between the parallel fibers and the Purkinje neuron dendrites in wild-type (WT) and Reeler mice. (A) Bundles of parallel fibers (**Pf**) in **WT** mice; two of them contact two Purkinje neuron dendrites (asterisks) and the synapses are segregated from the surrounding tissue by a well developed electron-lucent glial lamina (**Gl**), very close to a stellate neuron (**St**). Bar = 500 nm. (B) Bundles of parallel fiber (**Pf**), one of them contacting a Purkinje neuron dendrite (asterisk). Note the absence of the glial lamina. Bar = 250 nm. (C) Purkinje neuron dendrite (**Pd**) receiving a synapse at one spine (asterisk) from a parallel fiber (**Pf**) and one other synapse, from a climbing fiber (**Cf**) along its shaft. Bar = 250 nm. (D and E) Comparison of the ultrastructural features of the Purkinje neurons (**Pn**) in WT (D)

and Reeler (**E**) mouse. The polarization of the cell is immediately apparent in control animals where the Pn originates an upper dendritic trunk (asterisk) directed toward the molecular layer and displays a large cytoplasmic area totally devoid of organelles at its lower pole (double asterisks), corresponding to the origin of the axon hillock. Bar = 2 μm. (F) High magnification view of a small somatic spine on a Purkinje cell body (asterisk) in the Reeler. Bar = 250 nm. (G) Axo-somatic synapse between a Basket cell terminal (**Ba**) and the cell body of a Pn. Bar = 500 nm. (H) Axo-somatic synapse between a climbing fiber (**Cf**) and the cell body of a Pn. Bar = 500 nm. (I) A glomerulus formed by a central projection of a mossy fiber (**Mfr**) surrounded by several granule cell dendrites (**Gd**). The profile of the rosette is better differentiated than at P5, but still it is smoother than in WT mice. Bar = 250 nm. Abbreviations: Ba, basket cell; Cf, climbing fiber; Gd, granule cell dendrite (claw); Gl, glial lamina; Gr, granule cell; Mfr, mossy fiber rosette; P, postnatal day; Pd, Purkinje neuron dendrite; Pf, parallel fiber(s); Pn, Purkinje neuron; St, stellate neuron; WT, wild type.

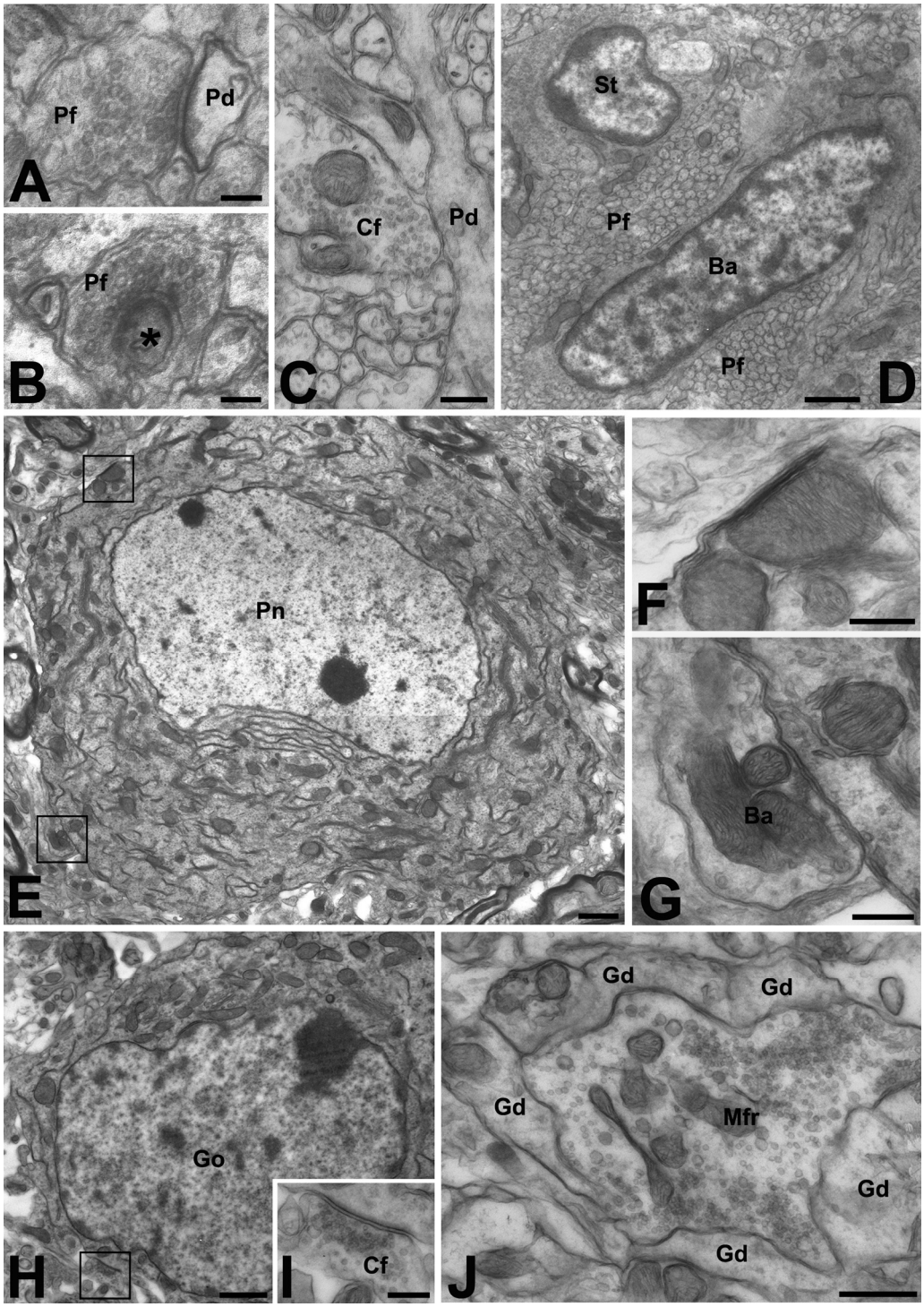

Fig. 7. Ultrastructure of the Reeler cerebellum at P15. (A–C) High magnification view of synapses in the molecular layer. (A) Synapse between a parallel fiber terminal (**Pf**) and a small Purkinje neuron dendrite (**Pd**). Bar = 100 nm. (B) Typical mature synapse between a parallel fiber terminal (**Pf**) and a Purkinje neuron dendritic spine (asterisk) that is now completely surrounded by the presynaptic axon. Bar = 100 nm. (C) The surface of a longitudinally cut Purkinje neuron dendrite (**Pd**) is still remarkably smooth with no evident spines. Bar = 250 nm. (D) Cells of the molecular layer are dispersed among the bundles of parallel fibers (**Pf**). A stellate (**St**) and a basket cell (**Ba**) are clearly recognizable. Bar = 1 μm. (E) Ultrastructure of a Purkinje neuron

(**Pn**) still retaining features of profound immaturity. The areas in the rectangles are shown at higher magnification in (F) and G. Bar = 1 µm. (F) Hypolemmal cistern, the typical membrane specialization of the Pn. Bar = 250 nm. (G) Typical axo-somatic synapse between the terminal of a basket cell (**Ba**) and the Pn cell body. Bar = 250 nm. (H) Typical Golgi cell with a round cell body and an unpolarized cytoplasm. The nucleus occupies the center of the cell. The area in the rectangle is shown at higher magnification in I. Bar = 1 µm. (I) Typical axo-somatic synapse between a climbing fiber terminal (**Cf**) and the soma of the Golgi cell. Bar = 250 nm. (J) A glomerulus formed by a central projection of a mossy fiber (**Mfr**) surrounded by several granule cell dendrites (**Gd**). The profile of the rosette is still smoother than in wild-type mice. Bar = 500 nm. Abbreviations: Ba, basket cell; Cf, climbing fiber; Gd, granule cell dendrite (claw); Go, Golgi neuron; Gr, granule cell; Mfr, mossy fiber rosette; P, postnatal day; Pd, Purkinje neuron dendrite; Pf, parallel fiber(s); Pn, Purkinje neuron; St, stellate neuron.

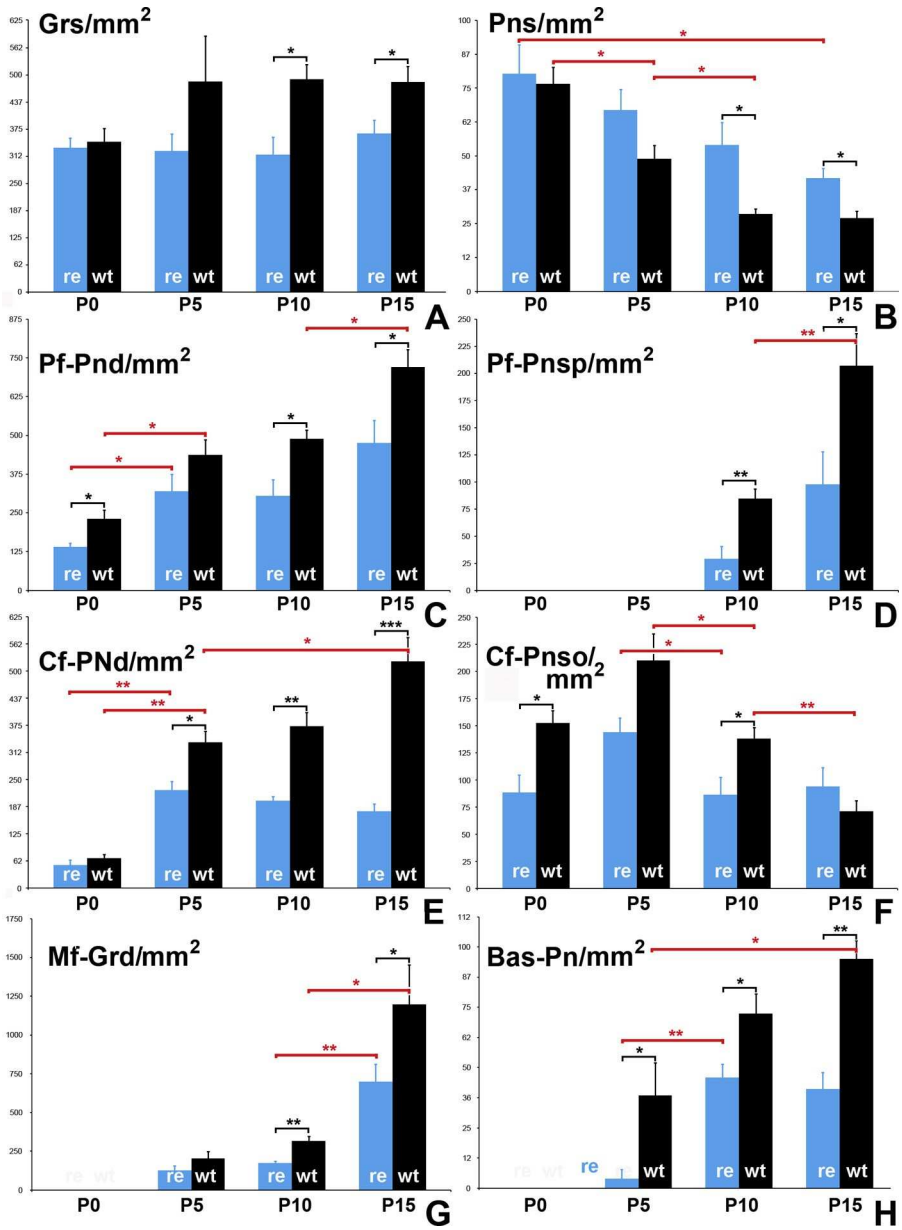

Fig. 8. Quantitative analysis of main ultrastructural changes in the postnatal cerebellar cortex of Reeler and wild-type (WT) mice. All data are expressed as object densities (n/mm^2). The density of granule cells (Grs;

A) is significantly reduced in Reeler mice compared to WT littermates starting from P10, whereas from the same developmental stage, the density of Pns (B) is significantly increased. Note, however, that there is a reduction by about one half in the density of Pns between P15 and newborn Reeler mutants (B). The densities of synapses between the parallel fibers and the Pn dendrites (Pf-Pnd; C) are statistically lower in Reeler than in WT mice at all post-natal ages except P5. Note that there is an increase in the density of these synapses at P0 and P5 and a substantial stabilization between P5 and P10 in both mutant and control mice. However, whereas in control mice the density of the Pf-Pnd contacts increases again, it only shows a positive tendency in Reeler without reaching statistical significance. The synapses between the parallel fibers and the dendritic spines of the Pns only appear at P10 (Pf-Pnsp; D) Also in this case, density is statistically lower in Reeler than in control mice and increases between P10 and P15 reaching statistical significance in WT but not in mutant mice. The densities of synapses between the climbing fibers and the Pn dendrites (Cf-Pnd) and soma (Cf-Pnso) are shown in (E) and (F), respectively. Only at birth, there is no statistically significant difference in the density of Cf-Pnd contacts between normal and mutant mice. In the P5–P15 interval Reeler mice constantly display a significant reduction in the densities of this type of synapse compared to WT mice. Whereas in the latter there is a net increase between P0 and P15 (with an apparent stability between P5 and P10), in Reeler the increase only occurs between P0 and P5. The density of Cf-Pnso contacts follows a less definite trend. (F) Whereas it is clear that in both mutant and control mice there is a significant reduction in the P5–P10 interval, comparison of Reeler and control mice at corresponding developmental stages indicates that although mutants have lower densities at birth, they eventually (P15) display figures not statistically different from controls. The contacts between the mossy fibers and granule cell dendrites (Mf-Grd; G) are detectable from P5 onward. Again their densities are lower in Reeler than in controls. In both phenotypes, however, there is a statistically significant increase from P10 to P15. The contacts between basket cells and the Pns (Bas-Pn; H) are detectable from P5 onward. In this case also their densities are lower in Reeler than in controls. In addition, whereas they increase with time in WT mice, they are only augmented in the P5–P10 interval in Reeler. Abbreviations: Bas, basket cells; Grs, granule cells; Cf, climbing fibers; Mf, mossy fibers; P, post-natal day; Pf, parallel fibers; Pnd, Purkinje neuron dendritic arborization (except spines); Pns, Purkinje neurons; Pnso, Purkinje neuron soma; Pnds, Purkinje neuron dendritic spines; re, Reeler; wt, wild-type. *$0.05 \leq p > 0.01$; **$0.01 \leq p > 0.001$; ***$p \leq 0.001$.

4. **Discussion**

4.1. Migration of Purkinje neurons and the granule cell-to-Purkinje neuron ratio

The ectopia of the Pns, which varies in degree, is the most salient architectonic anomaly of the Reeler cerebellum (Goffinet et al., 1984; Heckroth et al., 1989). In parallel, quantitative analysis of Pn number indicated that Reeler mice possess slightly less than half the number found in normal animals (Heckroth et al., 1989). Our ultra- structural observations not only confirmed the mispositioning of Pns, but also showed that, in mutant mice, these neurons retained a higher degree of immaturity. In addition, the limited number of neurons that succeeded in gaining a mature ultrastructure in Reeler displayed an altered horizontal orientation. This latter observation is in line with the recent demonstration by Miyata and colleagues (2010) that a Reelin deficit is responsible for an alteration in the migratory behavior of the Pns. These authors, by fluorescent tagging of the Pns in vivo and in slices, could only postulate the existence of anomalies in the development of the apical cytoplasmic swelling and the initial dendritic-like process. However, we can show here

that: (i) although the cytological features of the initial dendrite were comparable in Reeler and WT littermates, in the former it had a tendency to grow in a wrong direction; (ii) Reeler mice displayed an anomalous pattern of maturation of the axon together with the persistence of an unpolarized ultrastructure.

Heckroth and colleagues (1989) reported that adult Reeler mice possess approximately 82,000 Purkinje cells, slightly less than half the number found in normal mice. During normal cerebellar development, dying Pns were shown to be highly localized within the vermal midline in mouse, with a peak of apoptotic death at P3 (Jankowski et al., 2009). Cells with the typical ultrastructural features of apoptosis were seldom observed in our material. How- ever, whereas no differences in the density of Pns were observed between normal and mutated mice at P0–P5, the number of Pns/area remained significantly higher in Reeler at P10 and P15. Thus, our observations do not support the existence of a numerical reduction of Pns. However, it is possible that the increase in Pn density observed here results from volume (and hence section area) decrease of cerebellum in the mutants. The granule-to-Purkinje cell ratio is related to the degree of development and complexity of Pn arborization (Altman and Bayer, 1997). When densities of the granule cells and the Pns at P10 and P15 were averaged and their ratios calculated, control mice displayed a ratio 2.36 fold higher than mutants, in keeping with the previously demonstrated reduction in the complexity of the dendritic tree in Reeler (Kim et al., 2011).

4.2 Ultrastructure of the ML

The ML of the Reeler mouse in postnatal development retained much of the features that were encountered in WT mice, the only remarkable exception being the irregularities in distribution and differentiation of the radial glia, as previously shown in adult Reeler mutant mice after Golgi impregnation or tenascin immunostaining (Terashima et al., 1985; Yuasa et al., 1991).

After fractal analysis it was shown that, once the maximum complexity and fundamental tree pattern of the Pns are attained, the overall tree size further increases in direct relation to phylogenetic development (Takeda et al., 1992). However, no data were available until now on the presumptive synaptic modifications in the ML. The results of this work demonstrated that the types of synapses that are normally found in the ML of the normal cerebellum could also be identified in Reeler, although their degree of maturity was consistently attained at later postnatal stages.

Shaft junctions on the Pn dendrites are transient specializations suggested to possess the capacity to dissociate, and only a fraction of the parallel fibers forming shaft synapses with a developing Pn will establish spine synapses in the adult (Landis, 1987). Quantitative analysis showed that, in the P5–P10 interval, the densities of this type of contacts significantly increased in both control and mutant mice. They then continued to increase

only in WT mice in parallel with the appearance of mature synapses at spines. Both immature (shaft) and mature (spine) contacts displayed a significantly higher density in WT mice than in their mutant counterparts. These observations are consistent with the results obtained in mouse hippocampus (Borrell et al., 1999; Niu et al., 2004, 2008) and several areas of the forebrain in rat (Ramos-Moreno et al., 2006).

The process of climbing fiber pruning leads to perisomatic synapse elimination at P10–P15 in mouse (Watanabe and Kano, 2011). In keeping with these data, the synapses made by climbing fibers onto the Pn dendrites displayed higher densities in WT mice. These observations indicate that after an initial attempt (P0–P5) to follow the normal course of synaptogenesis, pruning was impaired, with the retention of some degree of immaturity. A very recent work, in keeping with the findings presented here, shows, although only at light microscopic level, that a deficiency of Dab2IP, a protein of the Reelin intracellular cascade, produced a number of cerebellar abnormalities such as a delay in the development of Pn dendrites, a decrease in the parallel fiber synaptic marker VGluT1, and an increase in the climbing fiber synaptic marker VGluT2 (Qiao et al., 2013).

4.3 Ultrastructure of the granular layers and central cellular mass of the postnatal Reeler mouse

Only minimal differences were detected between the ultrastructure of the EGL in Reeler and WT mice. They, first of all, reflected the reduction in number of the granule cells that is ultimately responsible for the hypocellularity of the mature granular layer leading to cerebellar atrophy (D'Arcangelo and Curran, 1998). Such a numerical reduction in mutants, from P10 onward, is indirectly confirmed here after quantitative analysis, when differences in granule cell densities between WT animals and their mutant litter- mates reached statistical significance. The IGL appeared to be more profoundly affected than EGL by the absence of Reelin, particularly regarding the neuropil organization that showed a quantitative reduction in the density of synaptic contacts made by mossy fibers at P10–P15.

A unique feature in Reeler is the persistence of the central cellular mass in the depth of the cerebellum. The cellular mass has been studied at light microscopy level and reported to be formed, for the most part, by mispositioned Pns. However, intermingled with the Pns there are also some other cells of various sizes and different ultrastructural characteristics. Our unpublished data after immunocytochemical labeling of Pns indeed showed the presence of large and medium-sized calbindin-negative neurons in the central mass. These were positioned to form the most medial part of the central mass and separated from the Pns by a strip of white mat- ter, with a pattern similar to what is observed in the rat cerebellar anlage at E19 (Altman and Bayer, 1997).

In conclusion, this study describes, for the first time, the postnatal development of the Reeler mouse cerebellum at ultrastructural level. Analysis of spatial and temporal modifications in architecture and cytological features during the first two postnatal weeks, a critical

period for the cerebellum to attain full maturation, not only confirmed the alterations previously observed after light microscopy and immunocytochemistry, but provided a detailed quantitative analysis of the trends and alterations in synaptogenesis.

References

Altman, J., Bayer, S.A., 1997. Development of the Cerebellar System. CRC Press, New York.

Borrell, V., Del Río, J.A., Alcántara, S., Derer, M., Martínez, A., D'Arcangelo, G., Nakajima, K., Mikoshiba, K., Derer, P., Curran, T., Soriano, E., 1999. Reelin regulates the development and synaptogenesis of the layer-specific entorhino-hippocampal connections. J. Neurosci. 19 (4), 1345–1358.

D'Arcangelo, G., Curran, T., 1998. Reeler: new tales on an old mutant mouse. Bioessays 20 (3), 235–244.

D'Arcangelo, G., Miao, G.G., Chen, S.C., Soares, H.D., Morgan, J.I., Curran, T., 1995. A protein related to extracellular matrix proteins deleted in the mouse mutant reeler. Nature 374 (6524), 719–723.

D'Arcangelo, G., Miao, G.G., Curran, T., 1996. Detection of the Reelin breakpoint in reeler mice. Brain Res. Mol. Brain Res. 39 (1–2), 234–236.

Falconer, D.S., 1951. 2 New mutants, trembler and reeler, with neurological actions in the house mouse (mus-musculus l). J. Genet. 50 (2), 92–201.

Goffinet, A.M., So, K.F., Yamamoto, M., Edwards, M., Caviness Jr., V.S., 1984. Architectonic and hodological organization of the cerebellum in reeler mutant mice. Brain Res. 318 (2), 263–276.

Heckroth, J.A., Goldowitz, D., Elsenman, L.M., 1989. Purkinje cell reduction in the reeler mutant mouse: a quantitative immunohistochemical study. J. Comp. Neu- rol. 279, 546–555.

Hellwig, S., Hack, I., Kowalski, J., Brunne, B., Jarowyj, J., Unger, A., Bock, H.H., Junghans, D., Frotscher, M., 2011. Role for Reelin in neurotransmitter release. J. Neurosci. 31 (7), 2352–2360.

Jankowski, J., Miething, A., Schilling, K., Baader, S.L., 2009. Physiological Purkinje cell death is spatiotemporally organized in the developing mouse cerebellum. Cerebellum 8 (3), 277–290.

Katsuyama, Y., Terashima, T., 2009. Developmental anatomy of reeler mutant mouse. Dev. Growth Differ. 51 (3), 271–286.

Kim, J., Kwon, N., Chang, S., Kim, K.T., Lee, D., Kim, S., Yun, S.J., Kim, J.W., Hwu, Y., Margaritondo, G., Je, J.H., Rhyu, I.J., 2011. Altered branching patterns of Purkinje cells in mouse model for cortical development disorders. Sci. Rep. 1 (122), 1–7.

Lambert de Rouvroit, C., Goffinet, A.M., 1998. The reeler mouse as a model of brain development. Adv. Anat. Embryol. Cell. Biol. 150, 1–106.

Landis, D.M., 1987. Initial junctions between developing parallel fibers and Pur- kinje cells are different from mature synaptic junctions. J. Comp. Neurol. 260 (4), 513–525.

Mariani, J., Mikoshiba, K., Changeux, J.P., Sotelo, C., 1977. Anatomical, physiological and Biochemical studies of the cerebellum from reeler mutant mouse. Proc. R. Soc. Ser. B 281, 1–28.

Mikoshiba, K., Nagaike, K., Kohsaka, S., Takamatsu, K., Aoki, E., Tsukada, Y., 1980. Developemental studies on the cerebellum from reeler mutant mouse in vivo and in vitro. Dev. Biol. 79, 64–80.

Miyata, T., Ono, Y., Okamoto, M., Masaoka, M., Sakakibara, A., Kawaguchi, A., Hashimoto, M., Ogawa, M., 2010. Migration, early axonogenesis, and Reelin-dependent layer-forming behavior of early/posterior-born Purkinje cells in the developing mouse lateral cerebellum. Neural Dev. 5, 23.

Niu, S., Renfro, A., Quattrocchi, C.C., Sheldon, M., D'Arcangelo, G., 2004. Reelin promotes hippocampal dendrite development through the VLDLR/ApoER2-Dab1 pathway. Neuron 41 (1), 71–84.

Niu, S., Yabut, O., D'Arcangelo, G., 2008. The Reelin signaling pathway promotes dendritic spine development in hippocampal neurons. J. Neurosci. 28 (41), 10339–10348.

Oostland, M., Buijink, M.R., van Hooft, J.A., 2013. Serotoninergic control of Purkinje cell maturation and climbing fibre elimination by 5-HT3 receptors in the juvenile mouse cerebellum. J. Physiol. 591 (Pt 7), 1793–1807.

Qiao, S., Kim, S.H., Heck, D., Goldowitz, D., LeDoux, M.S., Homayouni, R., 2013. Dab2IP GTPase activating protein regulates dendrite development and synapse number in cerebellum. PLoS ONE 8 (1), e53635, http://dx.doi.org/10.1371/journal.pone.0053635.

Ramos-Moreno, T., Galazo, M.J., Porrero, C., Martínez-Cerdeño, V., Clascá, F., 2006. Extracellular matrix molecules and synaptic plasticity: immunomapping of intracellular and secreted Reelin in the adult rat brain. Eur. J. Neurosci. 23 (2), 401–422.

Rice, D.S., Curran, T., 1999. Mutant mice with scrambled brains: understanding the signaling pathways that control cell positioning in the CNS. Genes Dev. 13 (21), 2758–2773.

Takeda, T., Ishikawa, A., Ohtomo, K., Kobayashi, Y., Matsuoka, T., 1992. Fractal dimension of dendritic tree of cerebellar Purkinje cell during onto- and phylogenetic development. Neurosci. Res. 13 (1), 19–31.

Terashima, T., Inoue, K., Inoue, Y., Mikoshiba, K., Tsukada, Y., 1985. Observations on Golgi epithelial cells and granule cells in the cerebellum of the Reeler mutant mouse. Brain Res. 350, 103–112.

Ventruti, A., Kazdoba, T.M., Niu, S., D'Arcangelo, G., 2011. Reelin deficiency causes specific defects in the molecular composition of the synapses in the adult brain. Neuroscience 189, 32–42.

Watanabe, M., Kano, M., 2011. Climbing fiber synapse elimination in cerebellar Purkinje

cells. Eur. J. Neurosci. 34 (10), 1697–1710.
Yabut, O., Renfro, A., Niu, S., Swann, J.W., Marín, O., D'Arcangelo, G., 2007. Abnormal laminar position and dendrite development of interneurons in the reeler forebrain. Brain Res. 1140, 75–83.
Yuasa, S., Kawamura, K., Ono, K., Yamakuni, T., Takahashi, Y., 1991. Development and migration of Purkinje cells in the mouse cerebellar primordium. Anat. Embryol. (Berl.) 184 (3), 195–212.
Yuasa, S., Kitoh, J., Oda, S., Kawamura, K., 1993. Obstructed migration of Purkinje cells in the developing cerebellum of the reeler mutant mouse. Anat. Embryol. (Berl.) 188, 317–329.